Photolysis of 1-aryl-3,3-dialkyltriazenes

Th. Lippert[a], J. Stebani[b], O. Nuyken[c], A. Stasko[d] and A. Wokaun[a,†]
[a]Physical Chemistry II, University of Bayreuth, D-95440 Bayreuth (Germany)
[b]Macromolecular Chemistry I, University of Bayreuth, D-95440 Bayreuth (Germany)
[c]Institute of Technical Chemistry, Technical University of Munich, D-85748 Garching (Germany)
[d]Department of Physical Chemistry, Slovak Technical University, 81237 Bratislava (Slovak Republic)

(Received May 21, 1993; accepted September 28, 1993)

Abstract

The photolytic decomposition of substituted 1-phenyl-3,3-diethyl-triazenes has been studied using both pulsed XeCl* excimer excitation at 308 nm, and continuous-wave irradiation with a xenon lamp. Electron-withdrawing substituents in the *para* position at the phenyl ring are found to decrease both the quantum yield of photolysis and the apparent first-order rate constant of decomposition. The reaction proceeds according to an overall one-step pathway; analysis of the photolysis products by gas chromatography–mass spectrometry is consistent with a radical decomposition mechanism.

For the compound 1-(4-nitrophenyl)-3,3-diethyl-triazene, an autocatalytic acceleration of the photolysis was observed during the continuous-wave irradiation, using a xenon lamp source. This phenomenon is analysed in terms of an involvement of the nitro group: photoreduction of the latter functionality involves the creation of solvent radicals in comparatively large concentrations, which are detected by *in-situ* electron spin resonance experiments. These radicals may attack and decompose further molecules of the starting material.

1. Introduction

Recently, substituted triazene derivatives R_1–N=N–NR_2R_3 have attracted considerable attention owing to their biological activity as cancerostatica [1] and herbicides [2], and their antitumor activity [3]. A novel application has been proposed on the basis of the strong UV absorption of triazenes at wavelengths around 300 nm, and their comparatively high thermal stability. These chromophores may be used as promotors for XeCl* excimer laser ablation of polymers which exhibit no intrinsic absorption at the wavelength of XeCl* emission [4]. During the photochemical cleavage of the triazeno group, nitrogen is released which acts as a driving gas in the laser-induced ablation process. Compared with standard techniques based on photoresists, the ablation of thin polymer layers offers the twofold advantage that neither a development step nor a transfer of the pattern from the resist into an underlying layer are required [5]: the structured polymer itself may remain on the substrate as a functional layer, as has been demonstrated for the case of polyimide.

High energy excimer lasers are increasingly being applied in microlithographic processes, in particular for the patterning of integrated circuits in the microelectronics industry [6]. Among the available UV lasers, the XeCl* excimer laser excels by high stability, ease and reliability of operation, and by a long lifetime of the employed gas mixture.

A first triazene compound was synthesized in 1862 [7]; a few years later the first 1-aryl-3,3-dialkyltriazene was prepared [8]. As an early application, the triazenes were used in the dye and textile industries [9], as a stabilized storage form for aromatic diazo compounds.

In view of the more recent applications mentioned, physicochemical characterization data of 1-aryl-3,3-dialkyltriazenes have been obtained from Raman spectroscopy studies [10], mass spectrometry [10], nuclear magnetic resonance (NMR) spectroscopy [11] and electron spin resonance (ESR) spectroscopy [12], from an investigation of protolytic decomposition [13], and from semiempirical quantum chemical calculations [14]. These compounds have recently been applied as sensitizers for the 308 nm excimer laser ablation of polymers [15].

Only a few studies have so far been concerned with the photolysis behaviour of triazenes.

†Author to whom correspondence should be addressed.

SSDI 1010-6030(93)03718-V

Fanghänel and coworkers [16] reported the (Z)–(E) isomerization of triazenes of the 1,2,3-triazabutadiene type (C–N=N–N=C). The (E) isomer was found to decompose to the corresponding diazonium salt during photolysis. Majer *et al.* [17] suggested an ionic mechanism for the photolysis of 1-aryl-3,3-dialkyltriazenes (with a morpholino residue as the *N*-dialkyl substituent), and gave indications for the involvement of a cis isomer as an intermediate. In their ground state, 1-aryl-3,3-dialkyltriazenes are known to exist in the more stable trans form from X-ray crystallography [18, 19].

For diphenyltriazene, a radical pathway of photolysis, competing with a *trans–cis* isomerization, has been reported in non-protic solvents [20]. A similar mechanism was derived from analysis of the products generated upon photolysis of various 1,3-bisaryl-3-alkyltriazenes [21], and of 1,3-bisaryltriazenes [22], including hetero-aryl compounds.

A radical pathway was also derived from an ESR study of the photolytic decomposition of 1-aryl-3,3-dialkyltriazenes [12]. The mentioned diversity of partly conflicting results suggested a more detailed study of the photolytic behaviour including kinetic investigations and product analysis, which are subjects of the present report.

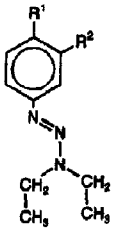

Scheme 1. Structural formula of investigated triazene compounds, as identified in Table 1.

TABLE 1. Investigated 1-phenyl-3,3-diethyl-triazenes

Compound label[a]	Substituents at phenyl ring	
	R^1	R^2
T 1/a	$N(CH_3)_2$	H
T 2/b	OCH_3	H
T 3/c	CH_3	H
T 4/d	H	H
T 5/e	Cl	H
T 6/f	CN	H
T 7	NO_2	H
T 8	H	NO_2
T 9/g	H	COOH
T 10/h	H	OCH_3

[a]Letters used in Fig. 4.

2. Experimental details

2.1. Photolysis and spectroscopy

A high pressure xenon lamp (150 W; LTI model A 1020) and a XeCl* excimer laser (Lambda Physik model LPX 120i) have been used as irradiation sources. The laser was operated at a pulse energy of 70–130 mJ, and a repetition rate of 2 Hz.

Photolysis experiments were carried out in quartz cuvettes. The solvents tetrahydrofuran (THF) (Aldrich; UV grade), benzene and *n*-hexane (Fluka; UV grade) were used without further purification. Solutions were carefully degassed with argon; concentrations were adjusted in the $(2\text{–}8)\times10^{-5}$ M range such that UV–visible spectra could be recorded without any further dilution of the solution on conventional spectrometers (Hitachi model U-3000, and Perkin–Elmer model Lambda 17).

Gas chromatography (GC)–mass spectroscopy (MS) analyses were carried out on a Finnegan mass spectrometer (MAT 312). EPR spectra were recorded on an X-band instrument (Bruker model EPR 200 D; $\nu_0=9.5$ GHz). Sample solutions, which had previously been degassed and were kept under argon, were irradiated *in situ* in the cavity of the EPR spectrometer, using a medium pressure mercury lamp (Applied Photophysics). Details of the experimental set-up and of the measurement conditions have been described elsewhere [12].

2.2. Materials

The investigated triazene compounds were synthesized according to the procedure described in detail elsewhere [11]. The general structural formula is shown in Scheme 1; the individual compounds, as distinguished by the substituents R^1 and R^2, are identified in Table 1.

3. Results

3.1. Excimer laser photolysis

During excimer laser irradiation of the triazene solutions, gaseous bubbles are observed to develop in the quartz cuvette at the front of the incoming laser beam, which are thought to be due to the nitrogen released during the photolysis. For each compound, the course of photolysis was followed by recording UV spectra off-line after a given number of XeCl* excimer laser pulses had been delivered to the sample. From the set of spectra thereby obtained, it was tested whether the pho-

tolysis proceeded in a simple one-step mechanism of type A→B, using the procedure of Mauser [23]. For all compounds, linear absorption difference diagrams with zero intercept were obtained. In agreement with the literature [20, 21], this suggests that photolysis proceeds by a mechanism as shown in Scheme 2; we note that the intermediate shown in parenthesis in the latter scheme is not detected on the time scale of our measurements.

From the usual analysis of the observed absorption differences (number of molecules decomposed per number of photons absorbed), the photolysis quantum yields have been determined for all the compounds investigated. These data may be used to compare the photochemical stability of the different triazenes and are compiled in Table 2. As a consistent trend among the set of *para*-substituted derivatives, T 1–T 7, the quantum yield is seen to decrease with increasing electron-withdrawing character of the substituent R^1. In our earlier study of bond orders in triazenes by semiempirical quantum chemical techniques [14], this behaviour has been attributed to the development of a 1,3-dipolar resonance structure, as will be discussed below.

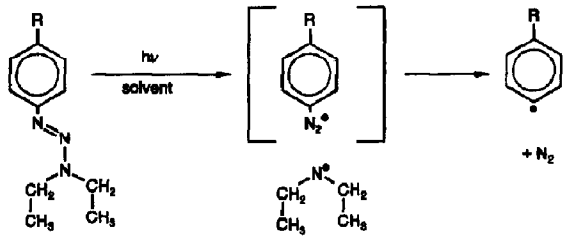

Scheme 2. General mechanism for the photolysis of 1-phenyl-3,3-dialkyl-triazenes.

The apparent quantum yield of the dimethylamino-substituted triazene T 1 is exceptionally high and is found to vary between 21 and 3% in the course of photolysis in THF solution (average value, 10.6%; *cf.* Table 2). This unusual behaviour is due to protolytic decomposition of this compound which proceeds in parallel with the photolysis, at pH ≤ 10. Our interpretation is supported by a detailed study of the protolysis kinetics reported elsewhere [13], and by the fact that largely different quantum yields are recorded in protonated and non-protonated solvents (methanol, 52%; cyclohexane, 10.2%; dimethylsulphoxide, 7.9%; in the latter solvent, a two-step decomposition of the type A→B→C is observed).

Test irradiations have also been performed at other wavelengths, *i.e.* at 248 nm (KrF* excimer laser) and at 350 nm (excimer-laser-pumped dye laser). Qualitatively, the same behaviour was found as described above, although different numerical values of the quantum yields were obtained.

3.2. *Photolysis by continuous-wave irradiation*

To obtain further insight into the kinetics of photolysis, continuous-wave experiments have been performed using a high pressure xenon lamp. The source was placed at a distance of 40 cm from the sample; filters were used to block the IR radiation. This set-up offers the advantage of very stable power (nominally 150 W at the source). Photolysis times were conveniently and precisely controlled by a mechanical shutter.

In the continuous-wave photolysis, a simple exponential decrease in absorption is seen for the

TABLE 2. Photophysical and photochemical parameters of investigated triazene compounds in tetrahydrofuran solution

Compound	Wavelength of absorption maximum λ_{max} (nm)	Molar extinction coefficient ϵ (M^{-1} cm^{-1})	Quantum yield of photolysis (%)	Rate constant of photolysis k (s^{-1})
T 1	351	19300	10.6[a]	1.82
T 2	289	12500	1.33	0.20
T 3	287	15300	0.6[a]	5.0×10^{-2}
T 4	285	15900	0.5[a]	2.8×10^{-2}
T 5	287	17900	0.4	9.4×10^{-3}
T 6	326	21100	0.36	1.4×10^{-3}
T 7	369	26700	0.48	–
T 8	291	19700	0.38	–
T 9	289	14200	0.48[a]	7.6×10^{-3}
T 10	314	13300	0.18	1.4×10^{-2}

[a]In the indicated cases the quantum yield was found not to be constant during the pulse experiments; an average over the entire course of photolysis is indicated. This effect is not due to quenching by photolysis products, as shown by the following experiment: when an aliquot of photolysis products was mixed into a fresh triazene solution, and the photolysis experiment was carried out in this mixture, the photolysis yield was found to be unchanged.

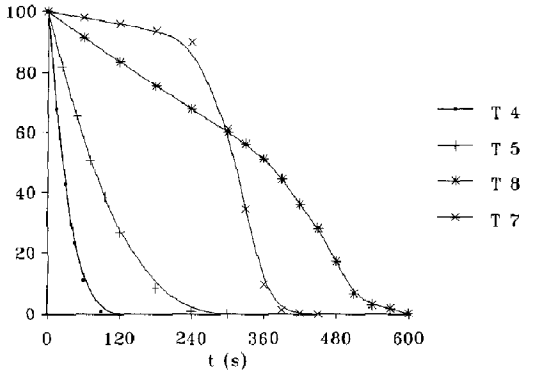

Fig. 1. Triazene photolysis in THF solution by irradiation with a high pressure xenon lamp, under the conditions described in the text. The UV absorption, measured at the respective maximum, is normalized with respect to its initial value (100%). The time dependence of the absorption is followed as a function of irradiation time for the triazene derivatives T 4, T 5, T 7 and T 8, as identified in Table 1.

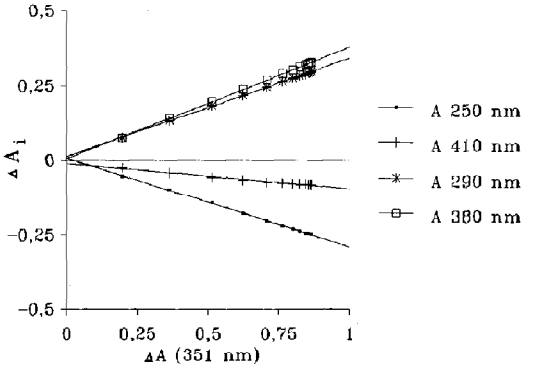

Fig. 2. Analysis of the reaction pathway according to Mauser [23], as exemplified for triazene T 1. Measured photolysis-induced absorption differences at various wavelengths, when plotted against the corresponding quantity ΔA at 351 nm, give rise to straight lines through the origin, showing that the reaction is of overall type A→B.

triazene derivatives T 4 and T 5 in Fig. 1. As had been found in the laser irradiation experiments, the absorption difference diagrams [23] indicate a simple one-step course (A→B) of the photolysis. This result is exemplified for compound T 4 in Fig. 2. A first-order analysis according to the Guggenheim [24] approximation has been used to calculate a rate constant k, which is included in Table 2. Absorbance values were recorded at equidistant times t_i during the photolysis. Absorption differences $\Delta A(t_i) = A(t_i) - A(t_i + \Delta)$ were calculated, where Δ is a fixed time increment on the order of two half-lives of the reaction. As prescribed by Guggenheim [24], a plot of $\ln[\Delta A(t_i)]$ *vs.* t_i yields a straight line, of slope k. Such a linear Guggenheim plot is illustrated for compound T 2 in Fig. 3(a).

The two nitro compounds T 7 and T 8 represent a remarkable exception. For these two compounds the decomposition is seen (Fig. 1) to accelerate after about 10% turnover for T 7, and after about 40% turnover for T 8. As a consequence, the Guggenheim plots for these two substances become highly non-linear, as illustrated in Fig. 3(b); it was not considered meaningful to extract a first-order rate constant. Interestingly, however, the absorption difference plots according to Mauser [23] are still linear, indicating that no intermediates are spectroscopically detected on the time scale of observation. Thus the overall reaction appears to be of type A→B, but the kinetics are distinctly different from first order. Possible origins for this behaviour will be discussed below.

Surveying the results for the entire series of compounds in Table 2, the apparent first-order rate constant k of photolysis is seen to be strongly influenced by the substitution pattern at the phenyl ring. A good linear correlation ($r = 0.98$) is obtained

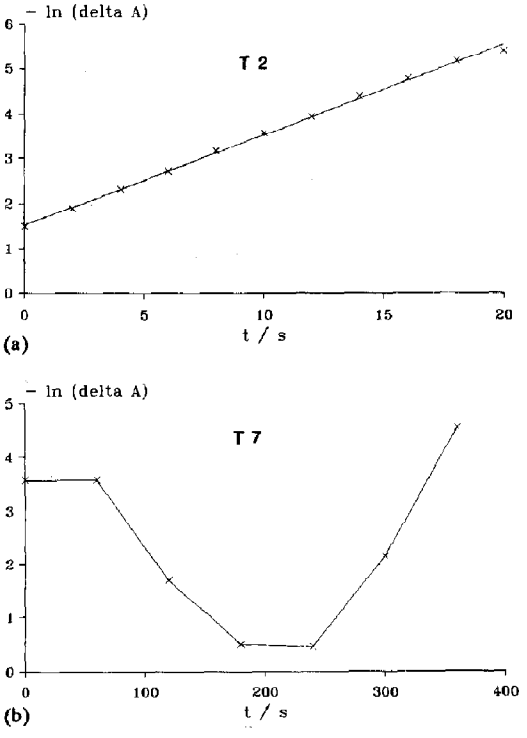

Fig. 3. "Guggenheim [24] plots" for triazene derivatives (a) T 2 and (b) T 7. The logarithm of the absorption difference $\Delta A(t_i) = A(t_i) - A(t_i + \Delta)$ is plotted against the photolysis time, t_i, see text.

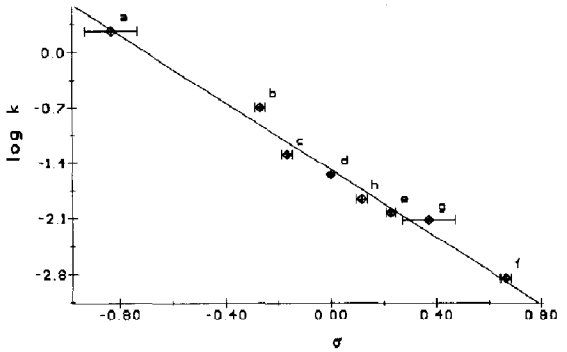

Fig. 4. Dependence of the apparent first-order photolysis rate constant k on the substitution pattern at the phenyl ring of 1-phenyl-3,3-diethyl-triazenes. A plot of $\log k$ (where k is in reciprocal seconds) against the Hammett parameter σ yields a linear correlation as shown by the full line ($\log k = -1.49 - 2.13\sigma$; correlation coefficient $r = 0.98$). Compounds are identified by labels a–h, as defined in Table 1.

if the logarithm of k is plotted against the Hammett [25] parameter σ, as shown in Fig. 4. For the slope ρ of the Hammett relation, a value of -2.13 is determined.

3.3. Product analysis

An analysis of the products generated upon excimer laser photolysis of triazenes T 6 and T 7 in benzene and n-hexane was carried out by GC–MS. Mass spectra were attributed to product molecules using several criteria: (i) a plausible assignment of the main fragmentation peaks in terms of the proposed structure; (ii) a high correlation of the observed spectrum with reference mass spectra of related structures from a data base [26]; (iii) possibility of generating the product from the parent compound using standard structural considerations.

Products derived from T 6 that have been identified in this manner are shown in Scheme 3. Approximate percentages have been indicated with the major products, to distinguish them from minority-product species. For many of the observed species, genesis may be explained in terms of the mechanism proposed in Scheme 2; the proposed routes of formation are indicated by arrows in Scheme 3. The main products are due to reactions of the substituted phenyl radical, generated by the triazene photolysis, with the solvent benzene, and with traces of water contained therein. Reaction products of the alkylamino radicals are also observed. Molecules containing acetyl groups (lower right-hand corner) may be formed from traces of ethylacetate in the solvent. Benzonitrile, if produced, would have remained hidden in the excluded volume of the GC–MS detection. (Because of its high boiling point, the solvent benzene is not quantitatively removed upon lyophilization of the photolysis product mixture and gives rise to a strong peak in GC when using UV detection.

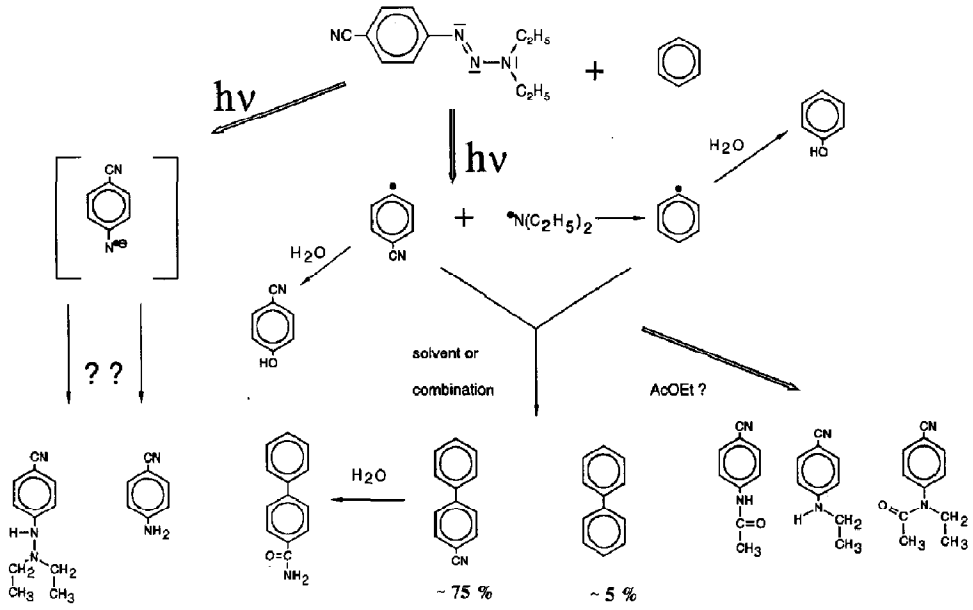

Scheme 3. Products generated during excimer laser photolysis of triazene T 6 in benzene solution, as identified by GC–MS analysis. Water and ethyl acetate are contained as traces in the benzene solvent.

Products that are eluted close to the solvent peak are omitted in the MS analysis.)

Products of the photolysis of T 7 in benzene (Scheme 4) may be derived from the same general mechanism, *i.e.* reaction of primary and secondary radicals with the solvent. Attention is drawn to the reduction of the nitro substituent, which yields an amino group in several of the products; this reaction will be discussed below. Two isomers of terphenyl are also observed.

In *n*-hexane solution, the variety of products from the photolysis of T 7 appears to be more complex, and assignment to the simple pathway of formation is difficult. A few structures that have been identified are shown in Scheme 5. Reaction products from the primary *N*-diethyl radicals with the solvent are detected in significant amount. (Although the latter species were not recorded with benzene used as a solvent (*cf.* Scheme 4), they might again have been hidden in the excluded volume of the GC–MS detection.)

3.4. Electron paramagnetic resonance investigations

To elucidate the mechanism leading to photoreduction of the nitro group observed with triazene T 7, a solution of this compound in CH_3CN was irradiated in the cavity of an ESR spectrometer, using the set-up and conditions described elsewhere [12]. The spin trap nitroso-durene (1-nitroso-2,3,5,6-tetramethyl-benzene) was added as a radical scavenger.

An electron paramagnetic resonance signal was observed to grow with increasing time of irradiation, as shown in Fig. 5. The multiplet displays a triplet structure (intensity ratio, 1:2:1) arising from a hyperfine coupling with two equivalent protons, with each multiplet component further split into three lines of equal intensity owing to hyperfine coupling with the nitrogen atom of the spin trap. This signal is attributed to the spin trap adduct of a $^{\bullet}CH_2CN$ radical from the solvent and thus proves the involvement of solvent radicals in the photolysis.

As a further test, we have tried to establish the formation of any nitroso-phenyl species involved in the photoreduction, by monitoring the UV spectrum *in situ* during the irradiation. Although no absorption was detected in the 700–800 nm range that would be characteristic of aromatic nitroso compounds, their presence cannot be excluded in view of the low values of the relevant molar extinction coefficients.

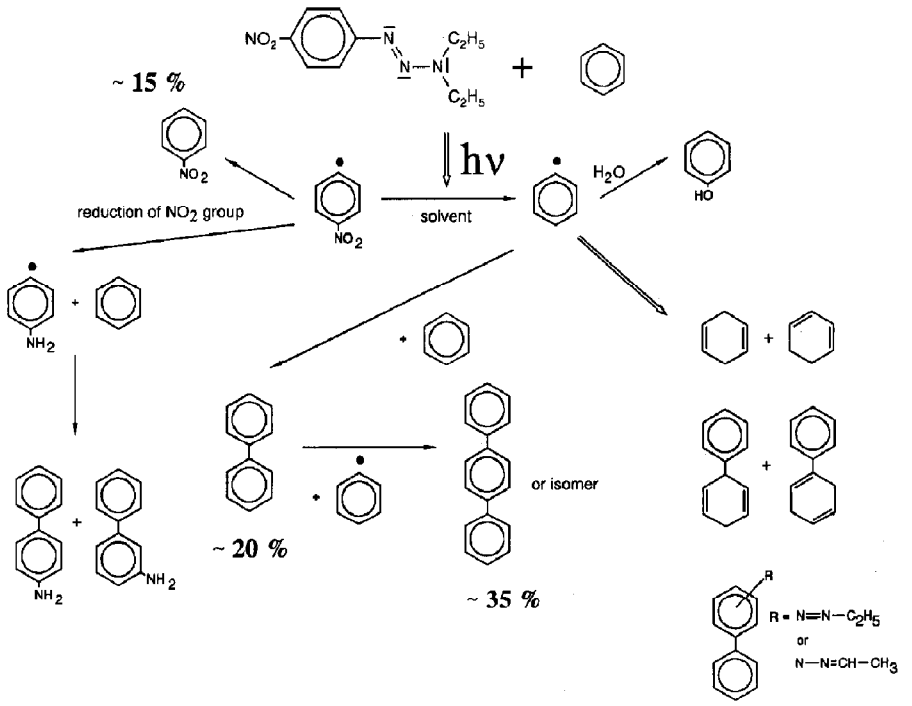

Scheme 4. Products generated during excimer laser photolysis of triazene T 7 in benzene solution, as identified by GC–MS analysis. Water is contained as traces in the solvent.

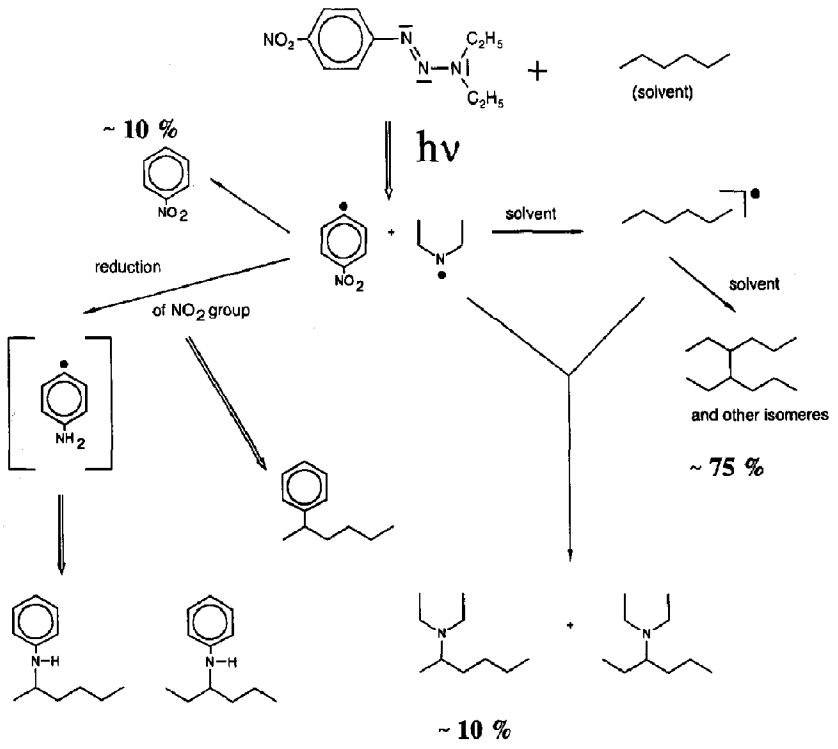

Scheme 5. Products generated during excimer laser photolysis of triazene T 7 in *n*-hexane solution, as identified by GC–MS analysis.

4. Discussion

Photolysis products identified are in agreement with the results of a recent ESR study [12], which gave evidence for a radical pathway of decomposition. This result is of importance in view of the recently demonstrated use of 1-phenyl-3,3-dialkyl triazenes as promoters for the excimer laser induced ablation of polymers, such as poly(methyl methacrylate). The radicals produced may induce "zip" depolymerization processes during laser ablation, which will result in a higher etch rate of ablation.

The apparent first-order photolysis rate constants show a good correlation with the Hammett parameter σ characterizing the substitution pattern at the aromatic ring. The established correlation opens the way for a tailoring of the photochemical stability of the triazenes, by a variation in the substitution pattern.

We note that the value obtained for the slope, $\rho = -2.13$, is quite similar to that determined for an analogous plot of the energy barriers to internal rotation, as determined from NMR measurements. For the latter case, a value $\rho = -1.95$ had been found [11]. In contrast, the protolytic decomposition of the triazenes appears to be significantly more sensitive to the substitution pattern. A Hammett plot of the apparent first-order rate constant against σ yielded a value $\rho \approx -5$ [13]. (The protolysis is catalysed by protonation of the triazene preceding the bond breakage. Therefore the overall rate is sensitive to the basicity of the polarizable triazeno group, and to the lability of the N^2–N^3 bond, which both respond in a sensitive manner to the introduction of electron-withdrawing substituents at the aromatic ring [13].)

In the photolysis of the nitro-substituted derivatives, linear absorption difference diagrams are observed as well, indicating that the reaction is of type A → B on the time scale of observation. However, the Guggenheim plots are non-linear, showing that the reaction is not of first order. From the shape of the time dependence, an autocatalytic type of decomposition process appears to take place. Evidence for a similar phenomenon has earlier been obtained in the photolysis of the structurally related azosulphonates [27]. An inspection of Table 2 also reveals that the quantum yield of T 7 is higher than expected from an extrapolation of the series T 2 → T 6, taking into account only the mesomeric effects of the *para*-positioned substituent R^1. This higher quantum yield hints to an involvement of the nitro group

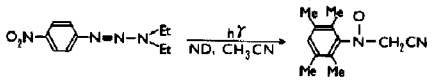

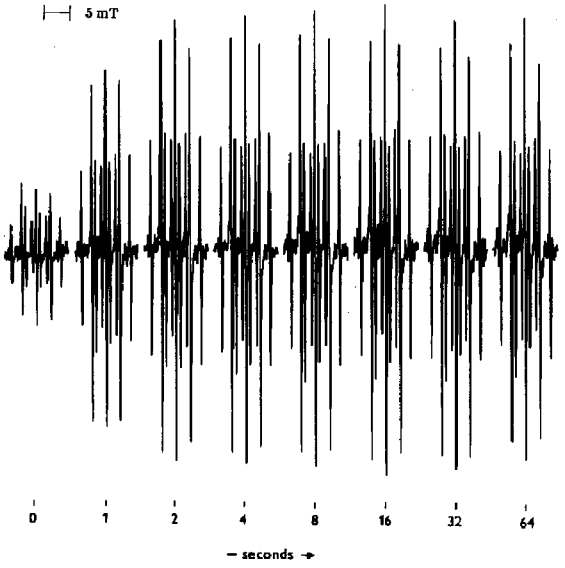

Fig. 5. *In-situ* photolysis of triazene T 7 (saturated solution in acetonitrile) in the cavity of an EPR spectrometer. The spin trap nitroso-durene was added at a concentration of 10^{-2} M. The observed signal is due to a spin trap adduct of the $^{\cdot}CH_2CN$ radical. The magnetic field scale is indicated by the calibration bar; relevant hyperfine couplings are $a_H(CH_2) = 0.977$ mT and $a_N(NO) = 1.342$ mT.

in the photolysis, which might be responsible for the autocatalytic acceleration of the decomposition.

Recent ESR results [28] on the photochemical decomposition of the pharmaceutical agent nifedipine, which contain a 2-nitro-phenyl group, are helpful in interpreting the anomalous behaviour observed for T 7. The photoexcited nitro group was found to abstract a hydrogen atom from the solvent, to form a radical of type R–NO$^{\cdot}$OH. Relevant steps of the mechanism derived in ref. 28 are summarized in Scheme 6. The R–NO$^{\cdot}$OH radical undergoes disproportionation into a nitro and a nitroso species. With further absorption of a photon and hydrogen abstraction from the solvent, the nitroso group is reduced to yield eventually the corresponding amine.

Transferring this mechanism to our present problem, we believe that the solvent radicals that are extensively created in the course of the photoreduction shown in Scheme 6 will attack further reactant molecules, thereby giving rise to an autocatalytic acceleration of the reaction. In the *in-situ* EPR experiments, production of the $^{\cdot}CH_2CN$ radicals from the solvent was only observed with triazene T 7. The intensity of the corresponding signal (Fig. 5) is already saturated after a time of about 2 s, *i.e.* 100 times faster than had been previously observed by one of us [28] with the nifedipine system. This is a strong indication that the concentration of photochemically produced radicals is high in the present case, supporting our above interpretation of the kinetic behaviour of triazenes T 7 and T 8.

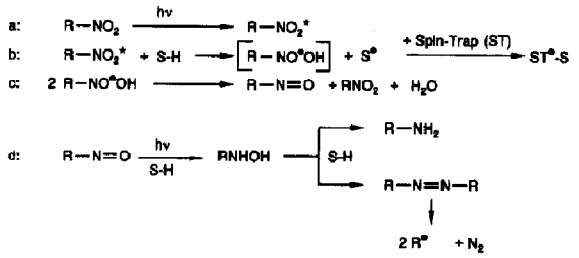

Scheme 6. Photoreduction of the nitro substituent at the phenyl ring involving product of radicals S$^{\cdot}$ from the solvent S–H (see text). Note that additional solvent radicals may be generated in step d.

It remains to be commented upon why, in contrast with the continuous-wave irradiation experiments just described, the pulse laser photolysis of T 7 yields a simple exponential decrease of absorption with the number of pulses. We recall that this is the only compound within the present series for which a significant difference between laser and lamp irradiations, *i.e.* a wavelength-dependent effect, is observed. From the analysis of the photolysis of the *p*-nitro-substituted derivative in hexane (Scheme 5), it may be noted that a large fraction of the primary phenyl radicals loses the nitro group in subsequent steps. The high photon energy of the laser may give rise to both a breaking of the bond between the phenyl ring and triazeno group, and detachment of the nitro group. Such an extensive decomposition, if occurring during each pulse, might result in an apparently simple overall decrease in the reactant concentration.

On the contrary, the "white" spectrum of the lamp contains significant spectral intensity at lower photon energies. Low energy photons may not be able to break the phenyl–triazeno bond at the beginning of the photolysis; instead, the nitro group would be excited. Thus the xenon irradiation source might induce a photochemical reaction pattern different from the one effected by the 308 nm photons of the excimer laser. This peculiarity may be a reason for the unusual time dependence observed during photolysis of T 7 and T 8 when

using xenon lamp irradiation. A wavelength-dependent photolysis behaviour has recently been demonstrated for substituted azosulphonates [29, 30].

An analysis of the photolysis product indicated in the lower left corner of Scheme 3 shows that the molecule may formally be derived from a 1,3-dipolar resonance structure. (The 1,3-dipolar structure indicates a partial charge shift within the triazeno group, as schematically represented by the equation

$$Phe\text{–}N^1{=}N^2\text{–}N^3(Et)_2 \leftrightarrow Phe\text{–}{}^{-}N\text{–}N{=}N^{+}(Et)_2$$

Evidence for this charge shift has been obtained from temperature-dependent NMR spectra [11] which show a hindered rotation around the N^2–N^3 bond. The barrier to rotation was assigned to a partial double-bond character of the latter bond, which was also confirmed by semiempirical quantum-chemical calculations [14]. Molecular orbital population analysis shows [14] that the relative contribution of the 1,3-dipolar structure amounts to about 10%. In the ESR spectra reported in ref. 12, radicals that may be derived from this structure have been detected.) For the substituted anilines shown in the bottom row of Scheme 5, genesis either from the 1,3-dipolar structure or from a photoreduced nitrophenyl radical can be conceived.

5. Conclusions

The photolysis rate of 1-phenyl-3,3-diethyltriazenes is strongly influenced by substitution at the aromatic ring. When the approximately white spectrum of a xenon lamp is used for continuous excitation, the overall rate constant of decomposition is increased by electron-donating and decreased by electron-withdrawing substituents in *para* position with respect to the triazeno group. This dependence may well be represented by a Hammett relationship, of slope $\rho = -2.1$. Quantum yields of photolysis determined by excimer laser irradiation, generally parallel the trends observed in the continuous-wave kinetics.

Deviations from simple first-order kinetics, *i.e.* an apparent acceleration of the reaction is detected during continuous-wave photolysis of the nitro-substituted triazenes. No intermediates other than reactant and final product(s) are spectroscopically detected in this case either. ESR investigations provided strong indications that a photoexcitation of the nitro group is involved, which is followed by hydrogen abstraction. As a consequence, a high concentration of solvent radical is detected *in situ*, which leads to an acceleration of the reaction due to radical attack on the parent molecule.

Acknowledgments

The authors are indebted to J. Reiner for help with the GC–MS analysis. Financial support of this work by grants of the Deutsche Forschungsgemeinschaft (SFB 213) and by the Verband der Chemischen Industrie is gratefully acknowledged.

References

1 H. Druckrey, *Xenobiotica, 3* (1973) 217.
2 R.E. McClure, Uniroyal Inc., *Br. Pat. 1, 130, 469; Chem. Abstr., 70* (1969) 19 788.
3 T. Giraldi, T.A. Connors and G. Carter (eds.), *Triazenes, Chemical, Biological and Clinical Aspects,* Plenum, New York, 1990.
4 T. Lippert, J. Dauth, O. Nuyken and A. Wokaun, in J.J. Pireaux, P. Bertrand and J.L. Bradas (eds.), *Polymer–Solid Interfaces,* Institute of Physics, Bristol, 1992, p. 391.
5 J.H. Brannon, *J. Vac. Sci. Technol., B, 7* (1989) 1064.
6 K. Jain, *Excimer Laser Lithography,* Society of Photo-Optical Instrumentation Engineers, Bellingham, WA, 1990.
7 P. Griess, *Justus Liebigs Ann. Chem., 121* (1862) 257.
8 A. Baeyer and C. Jäger, *Ber. Dtsch. Chem. Ges., 8* (1875) 148.
9 K. Venkataraman, *The Chemistry of Synthetic Dyes,* Vol. 1, Academic Press, New York, 1952.
10 F. Zimmermann, T. Lippert, C. Beyer, J. Stebani, O. Nuyken and A. Wokaun, *Appl. Spectrosc., 47* (1993) 986.
11 T. Lippert, J. Dauth, O. Nuyken and A. Wokaun, *Magn. Reson. Chem., 30* (1992) 1178.
12 A. Stasko, V. Adamcik, T. Lippert, A. Wokaun, J. Dauth and O. Nuyken, *Makromol. Chem.,* in press.
13 T. Lippert, J. Stebani, O. Nuyken and A. Wokaun, submitted for publication.
14 J.-C. Panitz, T. Lippert, J. Stebani, O. Nuyken and A. Wokaun, *J. Phys. Chem., 97* (1993) 5246.
15 T. Lippert, J. Stebani, O. Nuyken, J. Ihlemann and A. Wokaun, *Angew. Makromol. Chem.,* in press.
16 E. Fanghänel, J.U. Bauroth, H. Hentschel, F. Gußmann, H. Alzyadi and W. Ortmann, *J. Prakt. Chem., 334* (1992) 241; E. Fanghänel and J. Hohlfeld, *J. Prakt. Chem., 323* (1981) 253.
17 J. Majer, V. Rehak, J. Poskucil and L. Cihlo, *Wiss. Z. Tech. Hochsch. Leuna Merseburg, 16* (1974) 335.
18 F.R. Fronczek, C. Hansch and S.F. Watkins, *Acta Crystallogr., Sect. C, 44* (1988) 1651.
19 S. Neidle and D.E.V. Wilman, *Acta Crystallogr., Sect. B, 48* (1992) 213.
20 J. Baro, D. Dudek, K. Luther and J. Troe, *Ber. Bunsenges. Phys. Chem., 87* (1983) 1155.
21 M. Julliard, M. Scelles, A. Guillemonat, G. Vernin and J. Metzger, *Tetrahedron Lett., 4* (1977) 375.
22 M. Julliard, G. Vernin and J. Metzger, *Helv. Chim. Acta, 63* (1980) 467.
23 H. Mauser, *Z. Naturforsch., 23b* (1968) 1021.

24 E.A. Guggenheim, *Phil. Mag., 2* (1926) 538.
25 L.P. Hammett, *J. Am. Chem. Soc., 59* (1937) 96.
26 *Data Base for Mass Spectroscopy,* National Institute of Standard and Technology (NIST).
27 A. Stasko, O. Nuyken, B. Voit and S. Biskupic, *Tetrahedron Lett., 31* (1990) 5337.
28 A. Stasko, V. Brezova, S. Biskupic, K. Ondrias and V. Misik, *Mol. Pharmacol.,* in press.
29 D. Franzke, B. Voit, O. Nuyken and A. Wokaun, *J. Photochem. Photobiol. A: Chem., 68* (1992) 205.
30 D. Franzke, B. Voit, O. Nuyken and A. Wokaun, *Mol. Phys., 77* (1992) 397.